Journal of Physics: Conference Series **1342** (2020) 012010 doi:10.1088/1742-6596/1342/1/012010

Advanced Virgo Status

F. Acernese[50,17], T. Adams[26], K. Agatsuma[31], L. Aiello[10,16], A. Allocca[46,21], A. Amato[28], S. Antier[25], N. Arnaud[25,8], S. Ascenzi[49,23], P. Astone[22], P. Bacon[1], M. K. M. Bader[31], F. Baldaccini[45,20], G. Ballardin[8], F. Barone[50,17], M. Barsuglia[1], D. Barta[34], A. Basti[46,21], M. Bawaj[38,20], M. Bazzan[43,18], M. Bejger[5], I. Belahcene[25], D. Bersanetti[15], A. Bertolini[31], M. Bitossi[8,21], M. A. Bizouard[25], S. Bloemen[33], M. Boer[2], G. Bogaert[2], F. Bondu[47], R. Bonnand[26], B. A. Boom[31], V. Boschi[8,21], Y. Bouffanais[1], A. Bozzi[8], C. Bradaschia[21], M. Branchesi[10,16], T. Briant[27], A. Brillet[2], V. Brisson[25], T. Bulik[3], H. J. Bulten[36,31], D. Buskulic[26], C. Buy[1], G. Cagnoli[28,41], E. Calloni[42,17], M. Canepa[39,15], P. Canizares[33], E. Capocasa[1], F. Carbognani[8], J. Casanueva Diaz[25], C. Casentini[49,23], S. Caudill[31], F. Cavalier[25], R. Cavalieri[8], G. Cella[21], P. Cerdá-Durán[54], G. Cerretani[46,21], E. Cesarini[6,23], E. Chassande-Mottin[1], A. Chincarini[15], A. Chiummo[8], N. Christensen[2], S. Chua[27], G. Ciani[43,18], R. Ciolfi[13,24], A. Cirone[39,15], F. Cleva[2], E. Coccia[10,16], P.-F. Cohadon[27], D. Cohen[25], A. Colla[48,22], L. Conti[18], I. Cordero-Carrión[55], S. Cortese[8], J.-P. Coulon[2], E. Cuoco[8], S. D'Antonio[23], V. Dattilo[8], M. Davier[25], C. De Rossi[28,8], J. Degallaix[28], M. De Laurentis[10,17], S. Deléglise[27], W. Del Pozzo[46,21], R. De Pietri[44,19], R. De Rosa[42,17], L. Di Fiore[17], M. Di Giovanni[52,24], T. Di Girolamo[42,17], A. Di Lieto[46,21], S. Di Pace[48,22], I. Di Palma[48,22], F. Di Renzo[46,21], V. Dolique[28], M. Ducrot[26], D. Estevez[26], V. Fafone[49,23,10], S. Farinon[15], I. Ferrante[46,21], F. Ferrini[8], F. Fidecaro[46,21], I. Fiori[8], D. Fiorucci[1], R. Flaminio[28,29], J. A. Font[54,32], J.-D. Fournier[2], S. Frasca[48,22], F. Frasconi[21], V. Frey[25], L. Gammaitoni[45], F. Garufi[42,17], G. Gemme[15], E. Genin[8], A. Gennai[21], V. Germain[26], Archisman Ghosh[31], S. Ghosh[33,31], A. Giazotto[21], J. M. Gonzalez Castro[46,21], M. Gosselin[8], R. Gouaty[26], A. Grado[12,17], M. Granata[28], G. Greco[53,14], P. Groot[33], P. Gruning[25], G. M. Guidi[53,14], O. Halim[16,10], J. Harms[10,16], A. Heidmann[27], H. Heitmann[2], P. Hello[25], G. Hemming[8], T. Hinderer[33], D. Hoak[8], D. Hofman[28], D. Huet[25], G. Intini[48,22], J.-M. Isac[27], T. Jacqmin [27], P. Jaranowski[37], R. J. G. Jonker[31], F. Kéfélian[2], I. Khan[10,23], S. Koley[31], I. Kowalska[3], A. Królak[30,11], A. Kutynia[30], A. Lartaux-Vollard[25], C. Lazzaro[18], P. Leaci[48,22], M. Leonardi[52,24], N. Leroy[25], N. Letendre[26], M. Lorenzini[10,16], V. Loriette[9], G. Losurdo[21], D. Lumaca[49,23], E. Majorana[22], I. Maksimovic[9], N. Man[2], M. Mantovani[8], F. Marchesoni[38,20], F. Marion[26], A. Marquina[55], F. Martelli[53,14], L. Martellini[2], A. Masserot[26],

S. Mastrogiovanni[48,22], J. Meidam[31], M. Merzougui[2], R. Metzdorff[27], C. Michel[28], L. Milano[42,17], A. Miller[48,22], O. Minazzoli[2,7], Y. Minenkov[23], A. Moggi[21], M. Mohan[8], M. Montani[53,14], B. Mours[26], I. Nardecchia[49,23], L. Naticchioni[48,22], G. Nelemans[33,31], D. Nichols[33], S. Nissanke[33,31], F. Nocera[8], C. Palomba[22], F. Paoletti[21], A. Paoli[8], A. Pasqualetti[8], R. Passaquieti[46,21], D. Passuello[21], M. Patil[11], B. Patricelli[35,21], R. Pedurand[28,40], A. Perreca[52,24], O. J. Piccinni[48,22], M. Pichot[2], F. Piergiovanni[53,14], G. Pillant[8], L. Pinard[28], R. Poggiani[46,21], P. Popolizio[8], E. K. Porter[1], G. A. Prodi[52,24], M. Punturo[20], P. Puppo[22], P. Rapagnani[48,22], M. Razzano[46,21], T. Regimbau[2], L. Rei[15], F. Ricci[48,22], F. Robinet[25], A. Rocchi[23], L. Rolland[26], R. Romano[50,17], D. Rosińska[4,5], P. Ruggi[8], L. Salconi[8], N. Sanchis-Gual[54], B. Sassolas[28], P. Schmidt[33], D. Sentenac[8], V. Sequino[49,23,10], M. Sieniawska[5], A. Singhal[10,22], F. Sorrentino[15], G. Stratta[53,14], B. L. Swinkels[8], M. Tacca[31], S. Tiwari[10,24], M. Tonelli[46,21], A. Torres-Forné[54], F. Travasso[8,20], M. C. Tringali[52,24], L. Trozzo[51,21], K. W. Tsang[31], N. van Bakel[31], M. van Beuzekom[31], J. F. J. van den Brand[36,31], C. Van Den Broeck[31], L. van der Schaaf[31], J. V. van Heijningen[31], M. Vardaro[43,18], M. Vasúth[34], G. Vedovato[18], D. Verkindt[26], F. Vetrano[53,14], A. Viceré[53,14], J.-Y. Vinet[2], H. Vocca[45,20], R. Walet[31], G. Wang[10,14], M. Was[26], A. R. Williamson[33], M. Yvert[26], A. Zadrożny[30], T. Zelenova[8], J.-P. Zendri[18]

[1]APC, AstroParticule et Cosmologie, Université Paris Diderot, CNRS/IN2P3, CEA/Irfu, Observatoire de Paris, Sorbonne Paris Cité, F-75205 Paris Cedex 13, France
[2]Artemis, Université Côte d'Azur, Observatoire Côte d'Azur, CNRS, CS 34229, F-06304 Nice Cedex 4, France
[3]Astronomical Observatory Warsaw University, 00-478 Warsaw, Poland
[4]Janusz Gil Institute of Astronomy, University of Zielona Góra, 65-265 Zielona Góra, Poland
[5]Nicolaus Copernicus Astronomical Center, Polish Academy of Sciences, 00-716, Warsaw, Poland
[6]Museo Storico della Fisica e Centro Studi e Ricerche Enrico Fermi, I-00184 Roma, Italy
[7]Centre Scientifique de Monaco, 8 quai Antoine Ier, MC-98000, Monaco
[8]European Gravitational Observatory (EGO), I-56021 Cascina, Pisa, Italy
[9]ESPCI, CNRS, F-75005 Paris, France
[10]Gran Sasso Science Institute (GSSI), I-67100 L'Aquila, Italy
[11]Institute of Mathematics, Polish Academy of Sciences, 00656 Warsaw, Poland
[12]INAF, Osservatorio Astronomico di Capodimonte, I-80131, Napoli, Italy
[13]INAF, Osservatorio Astronomico di Padova, I-35122 Padova, Italy
[14]INFN, Sezione di Firenze, I-50019 Sesto Fiorentino, Firenze, Italy
[15]INFN, Sezione di Genova, I-16146 Genova, Italy
[16]INFN, Laboratori Nazionali del Gran Sasso, I-67100 Assergi, Italy
[17]INFN, Sezione di Napoli, Complesso Universitario di Monte S.Angelo, I-80126 Napoli, Italy
[18]INFN, Sezione di Padova, I-35131 Padova, Italy
[19]INFN, Sezione di Milano Bicocca, Gruppo Collegato di Parma, I-43124 Parma, Italy
[20]INFN, Sezione di Perugia, I-06123 Perugia, Italy
[21]INFN, Sezione di Pisa, I-56127 Pisa, Italy
[22]INFN, Sezione di Roma, I-00185 Roma, Italy
[23]INFN, Sezione di Roma Tor Vergata, I-00133 Roma, Italy
[24]INFN, Trento Institute for Fundamental Physics and Applications, I-38123 Povo, Trento, Italy
[25]LAL, Univ. Paris-Sud, CNRS/IN2P3, Université Paris-Saclay, F-91898 Orsay, France
[26]Laboratoire d'Annecy-le-Vieux de Physique des Particules (LAPP), Université Savoie Mont Blanc, CNRS/IN2P3, F-74941 Annecy, France

[27]Laboratoire Kastler Brossel, UPMC-Sorbonne Universités, CNRS, ENS-PSL Research University, Collège de France, F-75005 Paris, France
[28]Laboratoire des Matériaux Avancés (LMA), CNRS/IN2P3, F-69622 Villeurbanne, France
[29]National Astronomical Observatory of Japan, 2-21-1 Osawa, Mitaka, Tokyo 181-8588, Japan
[30]NCBJ, 05-400 Świerk-Otwock, Poland
[31]Nikhef, Science Park, 1098 XG Amsterdam, The Netherlands
[32]Observatori Astronòmic, Universitat de València, E-46980 Paterna, València, Spain
[33]Department of Astrophysics/IMAPP, Radboud University Nijmegen, P.O. Box 9010, 6500 GL Nijmegen, The Netherlands
[34]Wigner RCP, RMKI, H-1121 Budapest, Konkoly Thege Miklós út 29-33, Hungary
[35]Scuola Normale Superiore, Piazza dei Cavalieri 7, I-56126 Pisa, Italy
[36]VU University Amsterdam, 1081 HV Amsterdam, The Netherlands
[37]University of Białystok, 15-424 Białystok, Poland
[38]Università di Camerino, Dipartimento di Fisica, I-62032 Camerino, Italy
[39]Dipartimento di Fisica, Università degli Studi di Genova, I-16146 Genova, Italy
[40]Université de Lyon, F-69361 Lyon, France
[41]Université Claude Bernard Lyon 1, F-69622 Villeurbanne, France
[42]Università di Napoli 'Federico II,' Complesso Universitario di Monte S.Angelo, I-80126 Napoli, Italy
[43]Università di Padova, Dipartimento di Fisica e Astronomia, I-35131 Padova, Italy
[44]Dipartimento di Scienze Matematiche, Fisiche e Informatiche, Università di Parma, I-43124 Parma, Italy
[45]Università di Perugia, I-06123 Perugia, Italy
[46]Università di Pisa, I-56127 Pisa, Italy
[47]Institut FOTON, CNRS, Université de Rennes 1, F-35042 Rennes, France
[48]Università di Roma 'La Sapienza,' I-00185 Roma, Italy
[49]Università di Roma Tor Vergata, I-00133 Roma, Italy
[50]Università di Salerno, Fisciano, I-84084 Salerno, Italy
[51]Università di Siena, I-53100 Siena, Italy
[52]Università di Trento, Dipartimento di Fisica, I-38123 Povo, Trento, Italy
[53]Università degli Studi di Urbino 'Carlo Bo,' I-61029 Urbino, Italy
[54]Departamento de Astronomía y Astrofísica, Universitat de València, E-46100 Burjassot, València, Spain
[55]Departamento de Matemáticas, Universitat de València, E-46100 Burjassot, València, Spain

E-mail: antonino.chiummo@ego-gw.it

Abstract. The detection of a gravitational wave signal in September 2015 by LIGO interferometers, announced jointly by LIGO collaboration and Virgo collaboration in February 2016, opened a new era in Astrophysics and brought to the whole community a new way to look at - or "listen" to - the Universe. In this regard, the next big step was the joint observation with at least three detectors at the same time. This configuration provides a twofold benefit: it increases the signal-to-noise ratio of the events by means of triple coincidence and allows a narrower pinpointing of GW sources, and, in turn, the search for Electromagnetic counterparts to GW signals. Advanced Virgo (AdV) is the second generation of the gravitational-wave detector run by the Virgo collaboration. After a shut-down lasted 5 years for the upgrade, AdV has being commissioned to get back online and join the two advance LIGO (aLIGO) interferometers to realize the aforementioned scenario. We will describe the challenges and the status of the commissioning of AdV, and its current performances and perspectives.
A few lines wil be also devoted to describe the latest achievements, occurred after the TAUP 2017 conference.

1. Introduction

Advanced Virgo is the second generation of the Virgo detector for Gravitational Waves (GWs), built and operated by the Virgo collaboration, it is located in Cascina (Italy) at the European Gravitational Observatory (EGO) site. First generation of Gravitational Wave Interferometric

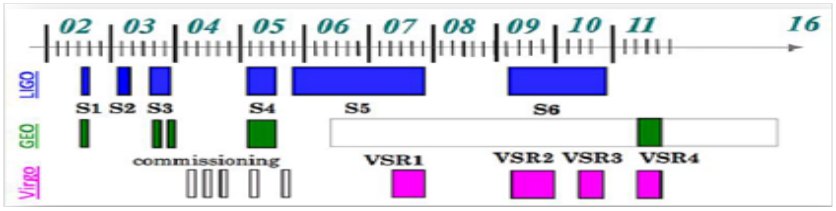

Figure 1. Timeline of the Science Runs for the first generation of Gravitational Wave interferometric antennas. Above scale indicates years since 2000.

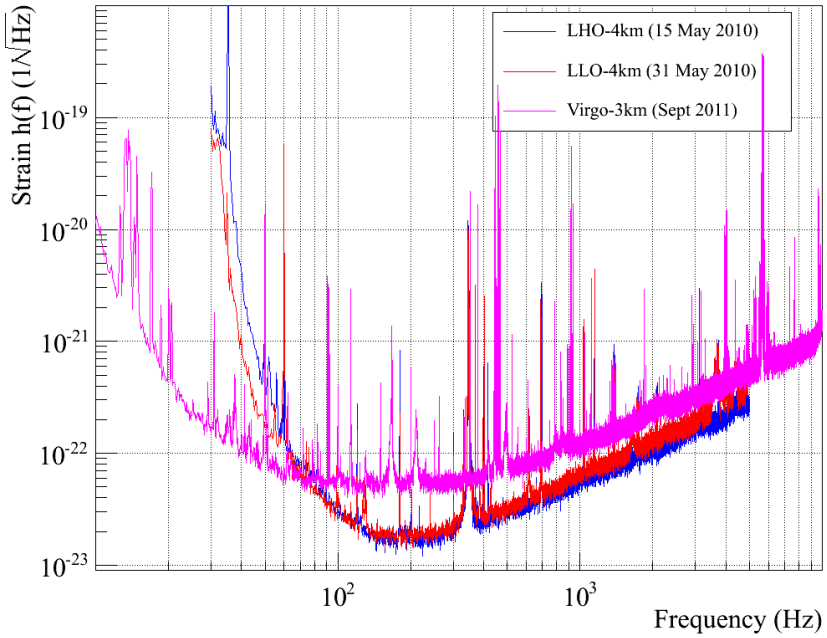

Figure 2. Strain sensitivities achieved by first generation LIGO and Virgo antennas at their best, before the shutdown to allow the upgrade to second generation.

Antennas (GWIAs) such as LIGO [1], Virgo [2] and GEO600 [3] operated for about one decade from 2002 to 2011. Those early instruments demonstrated a reliable and promising technology, an observing duty cycle up to 80% and a satisfactory stationarity of noise [4], and, probalby the most important outcome, they provided an excellent knowledge of limiting noise sources.
No detections were recorded during the first generation antennas science runs, nor was it really hoped to have any when the expected detection rate of $\sim$0.01 events per year is considered. Despite this huge limitation, a fair amount of Astrophysics results (examples in [5]) and of instrument development were made possible thanks to the experience of early generation.
Overall, thanks to the first generation of interferometric antennas, a clear path towards second generation antennas was developed [6].

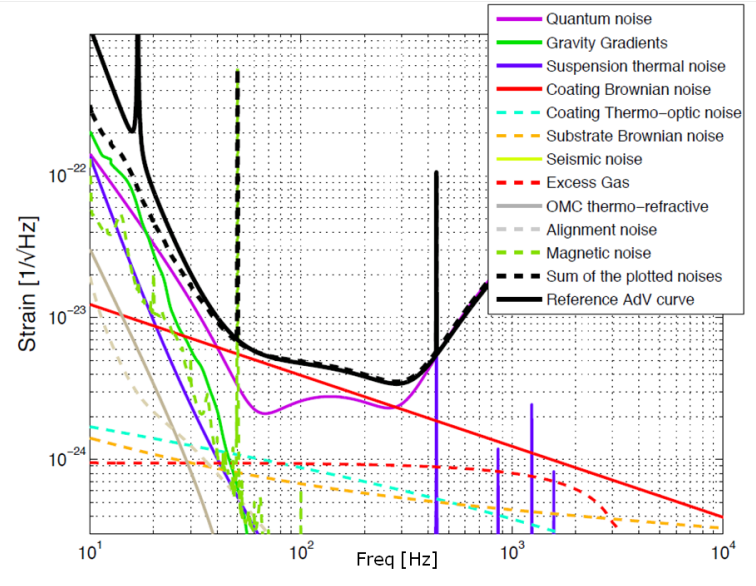

Figure 3. Limiting noises of the strain sensitivity at different frequency ranges for second generation antennas: example from Advanced Virgo technical design report [6]. Computation performed using GWINC code [8].

2. Beyond first generation

In order to achieve an expected detection rate which could make a detection likely to occur for the second generation antennas, strain sensitivity had to be improved by a factor ∼10, so to explore a volume of Universe roughly 1000 times larger and, in turn, make the expected detection rate of the order of some events per year of observation [7].

2.1. Limiting noises at different frequency ranges

The sensitivity to differential strain of the interferometer arms is limited by many noise sources, the most impacting are: newtonian noise, seismic noise, imperfect common technical noises cancellation at low frequency range [10-40Hz]; residual vibrations of both suspensions and mirror coatings due to environment thermal excitation, limiting at mid-frequency range [40-250Hz]; quantum shot noise at high frequency [250Hz-10KHz].
All of these noise sources had to be tackled to improve the sensitivity of the Advanced Detectors. In the following sections, we give an overview of the upgrades implemented in Advanced Virgo with respect to the initial Virgo detector.

2.2. Advanced Virgo design

Advanced Virgo topology is a dual-recycled, Fabry-Perot enhanced Michelson interferometer (see fig.4). It features 3km-long arms, Fabry-Perot cavities in the arms to enhance the GW-induced differential phase delay, and recycling mirrors at both the symmetric and antisymmetric ports [9]. The core optics (input and end test-masses, beam splitter, recycling mirrors) are suspended to superattenuators providing $\sim 10^{12}$ suppression of ground seismic motion.
Overall the design is similar to advanced LIGO (aLIGO) with some important differences, namely different technology for suspensions, shorter arms, marginally stable recycling cavities in central interferometer.

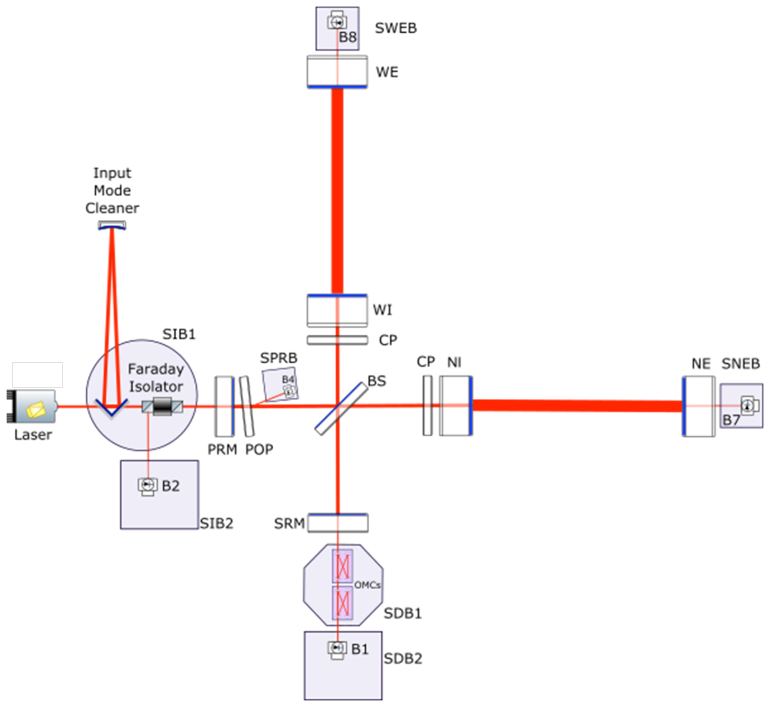

Figure 4. Advanced Virgo simplified optical layout. The test masses are indicated as W(N)I(E) short for West(North) Input(End). Power and Signal Recycling Mirrors (PRM, SRM) allow the recycling of either the injected power or the GW audio sidebands. The Input Mode Cleaner filters out residual higher order modes from the injected beam. The Compensating Plates (CPs) are shined by CO_2 laser with appropriate pattern to compensate for cold or thermally induced aberrations of the Optics. The input power will increase from current 15W to 125W of final configuration, and the Signal Recycling Mirror will be installed at a later stage.

2.3. Upgrades with respect to initial Virgo

The mid-frequency range [40-250Hz] is a region of interest for GW astrophysical sources such as Binary Neutron Stars (BNS) and, not surprisingly, it is where the ground-based GWIAs are most sensitive to the differential strain of their arms. Reducing thermal noise, the most offending noise in this range, is therefore mandatory. There are two main components of this kind of noise, the first is the mirror coating vibration, the second the vibrations of the suspensions of the mirrors. To reduce the latter, all kind of frictions and dissipations of mechanical energy have been reduced by using fused Silica monolithic suspensions to hang the test masses to their seismic superattenuators. The mitigation of the coating vibrations, instead, relies on enlarging the beam size at test-mass level, so probing a larger area of the mirrors and, in turn, averaging to a lower value the root-mean-square of the surface dynamical deformations.

The beam size on the Test Masses of Advanced Virgo has been increased by a factor 2.5 with respect to initial Virgo, with an expected mitigation of coating thermal noise by roughly the same factor.

The increase in size of the laser beam on the test masses is probably the upgrade to Advanced Virgo which implied the largest impact on the initial Virgo infrastructure and topology. Indeed, in order to accomodate this larger beam, most of the vacuum link pipes in the central area (as opposed to the long pipes in the arms) had to be replaced with larger ones, more demanding mode matching telescopes had to be developed and more difficult-to-operate, quasi-symmetrical Fabry-Perot cavities were installed in the arms. The largest impact was anyway on the Recycling

Cavities which, to be accomodated in the existing buildings, had to be designed with a very small Gouy phase, of the order of few milliradians, becoming only marginally stable [6].

Due to the reduced Gouy phase in the recycling cavities, Thermal Compensation System (TCS) of the optical aberrations is expected to play a major role in keeping the interferometer at the designed working point and suppressing the scattering of the main mode to higher order modes. This system has been greatly enhanced with respect to initial Virgo. Test masses are all equipped with ring heaters to correct for radius of curvature discrepancies, CO_2 laser can project different patterns onto the dedicated optics (compensation plates) to provide compensations of thermally induced deformations and cold aberrations. Appropriate sensors such as Hartmann wavefront sensors and phase cameras have been put in place to provide monitor signals for these aberrations.

The residual gas pressure noise has been also mitigated by reducing further the vacuum pressure in the 3km-long tubes from 10^{-7} mbar of intial Virgo to 10^{-9} mbar.
One of the worst offending noise at low-to-mid frequency range is due to stray light (ghost beams, scattered light, etc.) probing vibrations of mechanical structures and then recombining to the main beam of the interferometer. A new set of baffles of different shapes and materials has been put in place during the upgrade to Advanced Virgo, able to intercept and dump most of the predicted stray light. Furthermore, critical photodiodes have been installed on suspended optical benches in vacuum, to reduce as much as possible the displacement noise of the light scattered off the sensors and recombining to the main beam.

The quantum nature of light plays a role in the noise sensed by GWIAs both at low and high frequency range. The amplitude quantum noise is responsible for radiation pressure noise and is more evident at low frequency, but many other technical noises could be dominant in this range. Quantum noise on the phase of the fields, instead, actually limits the sensitivity in the region 300Hz - 10KHz (shot noise). In order to mitigate this noise, the arm Fapry-Perot cavities have an increased Finesse (roughly 9 times larger than initial Virgo) and the injected laser power is designed to be $\sim$16 times larger than in Virgo. Radiation pressure noise has been mitigated by using test masses twice as heavy (40Kg) as in Virgo.

Both coating materials and process on one side, and substrate materials of the core optics on the other have been improved with respect to the first generation Virgo. The four mirrors forming the two arm cavities, along with the Beam Splitter (BS) are the most critical optics of the interferometer. The cavity mirrors have a diameter of 350mm and a thickness of 200mm, while the BS mirror has a 550mm diameter and 35mm thickness. The different optical losses such as scattering or absorption have to be kept at a very low level. To achieve that, not only the substrate of the mirrors is made of the purest fused silica glass available, but also the polishing which gives the shape of the surface is done at the atomic level with on the central part, a peak to valley of the height of the mirror surface consistently less than 2 nm. Finally, the coating at the same time of each couple of test masses (either the two input mirrors or the two end mirrors) ensured a very good symmetry, and, in turn, a remarkable cancellation of common noises in the interferometer when operated at dark fringe.

3. Integration issues

The integration phase of all the components of Advanced Virgo has been accompanied by many small annoyances and big troubles: all of them had to be tackled to ensure a proper functioning of the new interferometer. The most concerning were the failures of some Superattenuator maraging steel blades and of monolithic suspensions.

3.1. Superattenuator maraging blade failures
Superattenuator hardware had worked for longer than 10 years without relevant issues when, preparing for the accomodation of new payloads, some of the maraging steel blades were found faulty - subsequent investigations showed because of embrittlement due to Hydrogen contamination during the machining process. At that point it was mandatory to perform inspection of the status of all the blades and, as a consequence of the findings, replace 40% of all of them (as a precaution).

3.2. Breaking of the monolithic suspension fibers
Monolithic suspensions were already successfully demonstrated during the Virgo Scientific Runs VSR3/4 (2010-11), so no issues were expected from this side. Instead, quite surprisingly, repeated breaking of monolithic suspension fibers under vacuum occurred during installations on 2015-2016. Throughout investigation was therefore triggered to find the causes of failure and possible solutions. The failure of glass anchors was soon excluded by microscope analysis of fractures, since the breaking always occurred at the level of the fibers. Basic mechanism of fiber breaking under vacuum was eventually identified: fast dust particles hit the fiber and produce fractures, then evolve with different rate to a full break. The origin of the dust was finally identified in some scroll pumps now to be deeply modified. Temporary solution, driven mainly by schedule considerations, was to fall back to steel wires for payloads. Sensitivity with steel wires has been calculated to be still compatible with the goal for the early stage of Advanced Virgo.

4. Advanced Virgo early-stage
In this section the status of Advanced Virgo, as of July 2017, is described, when the goal was to join Advanced LIGO in the second part of Observation Run 2 (O2).
Basically the commissioning of the interferometer starts when last component has been integrated and the main purpose is to bring the interferometer to the designed working point.

4.1. Commissioning
Due also to the monolithic suspension issue, the whole interferometer was not available for commissioning before October 2016. Since the second, and last, part of O2 was scheduled to start in August 2017, this left only ten months to go from scratch to an acceptable sensitivity for Advanced Virgo. The first one hour long lock of the interferometer at what is called *dark fringe* working point was achieved in six months, on March 2017, and marked a major project milestone.
First AdV commissioning run (termed *C8*) occurred from May 5th to 8th, and it was the first opportunity to monitor the whole instrument for some days. Then an engineering run (ER11) was held in June '17 in coincidence with aLIGO: first part from 16th to 19th with a BNS range varying from 5 to 9Mpc, and a duty cycle $\sim$70%, second part from 23rd to 26th with a BNS range $\sim$8-9Mpc, duty cycle $\sim$80%.
While the duty cycle was quite satisfactory, the BNS range was too low to really hope to join O2 on time. So, after ER11 an even more intense campaign was launched to achieve a sensitivity allowing to contribute to the science of aLIGO observing run: investigation on stray light, noise injections (magnetic, acoustic, seismic, etc.) to understand coupling from the environment to the interferometer, switch-off tests of selected devices. All of these activities helped in pinpointing criticalities and finding solutions to noise couplings. Furthermore, some room for optimization of Data Acquisition pipeline and read-out was still left, and for lock robustness improvement (alignment, loop accuracy, etc.) as well.
In the end efforts payed off: the longest lock segment was of the order of $\sim$20hrs (before O2:

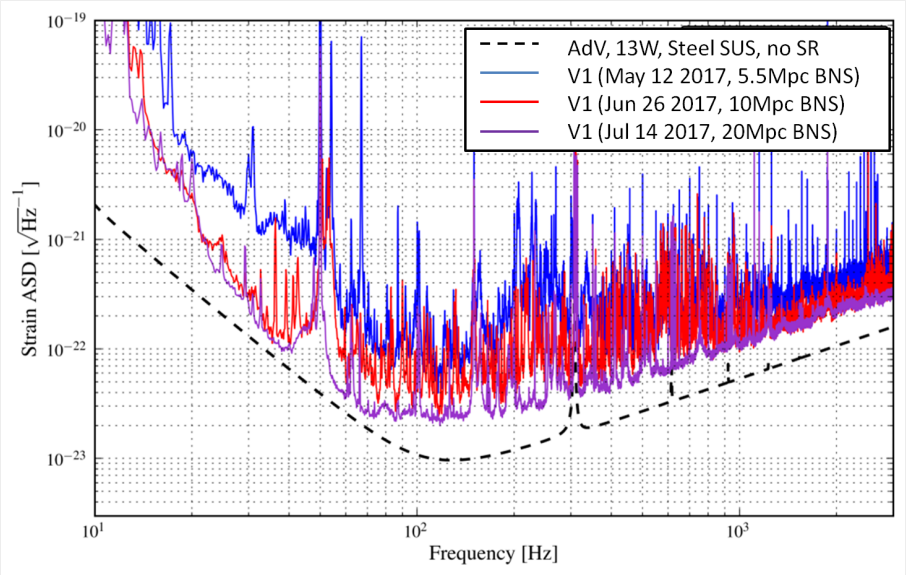

Figure 5. Evolution of the strain sensitivity during the commissioning of AdV, before joining the Observation Run 2 (O2).

it has been around 70hrs during O2), the unofficial milestone of beating initial Virgo best sensitivity was soon reached and the BNS range topped at 20Mpc just a couple of weeks before joining O2 (then it would have reached a maximum value of around 30Mpc during O2), enough to contribute to science data as part of the network of three interferometers.

One of the most relevant tool during the investigation of noises was the *Noise Budget* tool, a modellization of the interferometer with either measured or simulated transfer functions from different noises to the strain sensitivity. Thanks to this tool, a noise breakdown was possible, and this gave the commissioners an important indication about the criticalities to tackle. Before O2, most of the noises limiting the sensitivity were indeed well understood, although some peaks still remained to be explained (see fig. 6). A new campaign for the mitigation of known noises was already foreseen before O2 and actually started after the end of the run.

4.2. Optical characterization

In order to proper modelize the behavior of the interferometer, an extensive measurement campaign to characterize optical parameters was carried out. The arm cavities characterization gave round-trip losses (RTL) compatible with the design value (<75ppm) and quite balanced. Also the Finesse values of the two arms were compatible with nominal values, and as a result, a very low contrast defect of ∼8 ppm was measured, when compensated for the intentional offset between the two arm locking points (DC readout [6]). The Optical parameters are therefore very close to nominal.

Despite the fact that the power recycling cavity (PRC) is marginally stable and so rather prone to ricirculate also high order modes (HOMs), there has been no need of TCS actions before the O2 run. Actually, all the fields ricycled inside the PRC experience a gain close to the design value and anyway well predicted by simulations.

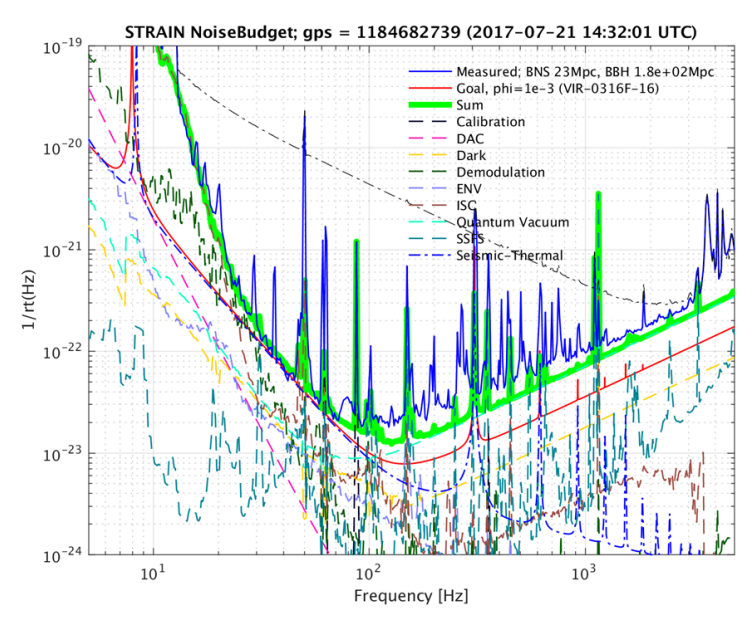

Figure 6. Noise budget of AdV strain sensitivity, before joining the Observation Run 2 (O2). Most of the noises were well understood, although additional investigations were needed to understand the origin or the couplings of unexplained limiting noises.

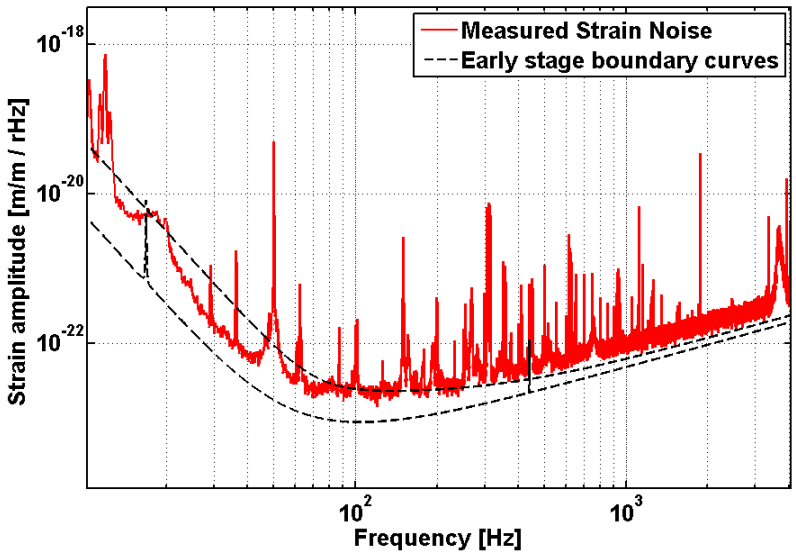

Figure 7. The strain sensitivity curve (solid red) as measured few days before AdV joined O2 data-taking, compared with the target curves (black dashed) for early-stage AdV configuration as computed in [10].

5. Summary and perspectives

Advanced Virgo is now fully operational, and this permitted to join aLIGO for the second part of the O2 run (August 1st to 25th), a major achievement. Many issues have still to be

addressed, but significant progress has been made. For instance, the monolithic suspension had to be replaced with metallic wires to increase reliability, but origin of the failing was eventually understood and countermeasure designed. The optical parameters of the interferometer are very close to nominal values, so that an excellent rejection of common mode noises can be achieved. On the lenght sensing and control (LSC) side, the lock acquisition proved to be robust and reliable (with lock segments lasting tens of hours before O2, and days during O2).
The strain sensitivity has been brought very close to early-stage target defined already in 2013 [10], as reported in fig.7, and, probably even more important, most of the limiting noise sources have been identified (see fig.6). This means that the post O2 commissioning phase has a clear path about what to address to enhance AdV sensitivity.
The activities already foreseen to prepare AdV for next data-taking jointly with aLIGO are: vacuum system upgrade for dust protection, monolithic suspensions re-installation, high power laser installation, more noise-hunting (stray light issues, data-acquisition hardware configuration, etc), parameters tuning with TCS. Also planned during that period is the installation of a squeezed vacuum field source at the output of the detector[11]. This device, provided by the Albert Einstein Institute in Germany, allows to improve the sensitivity in the high frequency range by engineering the quantum fluctuation of the vacuum field entering the dark port of the detector.

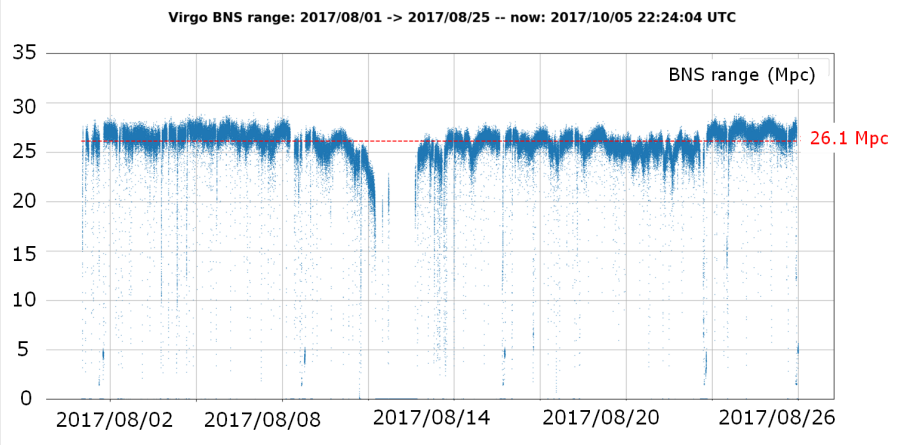

Figure 8. Plot of the AdV range for Binary Neutron Star Mergers as GW sources during O2 data-taking. Average value was around 26Mpc, with a maximum value exceeding 28Mpc.

6. Recent updates

The joint observation run with aLIGO and AdV started days after TAUP conference 2017, so most of what reported hereby do not cover the data-taking period. During the run the AdV detector had a duty cycle of 86% in science mode, with an average BNS range of ∼26Mpc. The importance of a three-detector network was soon evident during the run. Advanced Virgo, as part of the network, detected at least two GW signals for which it was possible to significantly restrict the uncertainty area on the celestial sphere associated with gravitational waves signals. The first ever triple coincidence signal *GW170814* was from a Binary Black-Hole merger [12], while the second, coded *GW170817*, came from a BNS merger. In this latter case, the directionality of the three-detector response allowed to send quite accurate a trigger to optical telescopes and permitted the discovery of an electromagnetic counterpart of the GW source [13]. Multi-messenger Astronomy has officially begun.

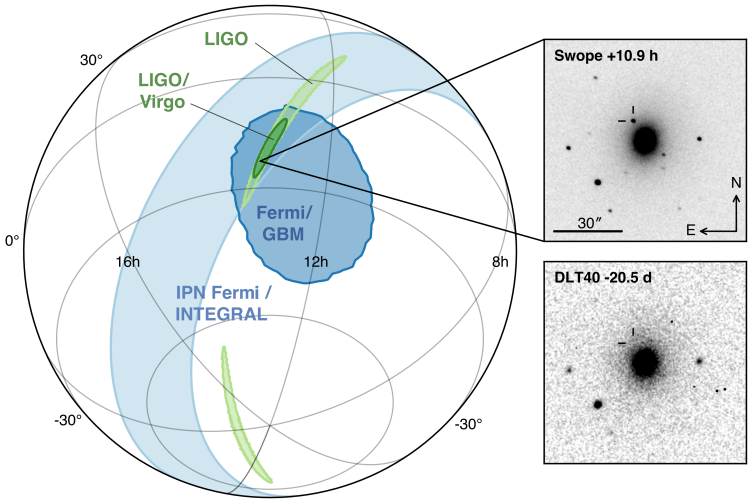

Figure 9. The participation of a third detector to the GWIAs network allowed the prompt pinpointing of the direction of arrival of the signal coded GW170817. This served as a trigger for electromagnetic telescopes which were able to detect the optical counterpart of the GW source in the Galaxy NGC4993. In the pictures, NGC4993 before (bottom) and after (top) the detection of GW170817 by aLIGO and AdV [13].

References

[1] Abbott B P, et al. 2009 LIGO: the Laser Interferometer Gravitational-Wave Observatory *Rep. Prog. Phys.* **72** 076901
[2] Accadia T et al 2012 Virgo: a laser interferometer to detect gravitational waves *JINST* **7** P03012
[3] Wilke B et al. 2002 The GEO 600 gravitational wave detector *Classical and Quantum Gravity* **19** 1377
[4] The LIGO Scientific Collaboration, The Virgo Collaboration 2012 Sensitivity Achieved by the LIGO and Virgo Gravitational Wave Detectors during LIGO's Sixth and Virgo's Second and Third Science Runs *Preprint* arXiv:1203.2674 [gr-qc]
[5] Abbot B P, et al. 2009 An upper limit on the stochastic gravitational-wave background of cosmological origin *Nature* **460** 990
[6] Accadia T et al 2012 Advanced Virgo Technical Design Report *Virgo Technical documentation system* **VIR-0128A-12** url: https://tds.virgo-gw.eu/ql/?c=8940
[7] Abbott B P, The LIGO Scientific Collaboration, Virgo Collaboration et al. 2016 *Living Rev Relativ* **19** 1 https://doi.org/10.1007/lrr-2016-1
[8] Gravitational Wave Interferometer Noise Calculator, available at https://awiki.ligo-wa.caltech.edu/aLIGO/GWINC
[9] Acernese F et al. 2014 Advanced Virgo: a second-generation interferometric gravitational wave detector *Classical and Quantum Gravity* **32** 024001
[10] Abbot B P et al. 2013 Prospects for Localization of Gravitational Wave Transients by the Advanced LIGO and Advanced Virgo Observatories *Preprint* arXiv:1304.0670v1 [gr-qc]
[11] Chua S, Slagmolen B, Shaddock D, and McClelland D 2014 *Class Quantum Grav* **31**, 183001
[12] Abbot B P, et al. 2017 GW170814: A Three-Detector Observation of Gravitational Waves from a Binary Black Hole Coalescence *Phys. Rev. Lett.* **119** 141101
[13] Abbot B P, et al. 2017 Multi-messenger Observations of a Binary Neutron Star Merger *The Astrophysical Journal Letter* **848** L12